MARTIN MARIETTA ENERGY SYSTEMS LIBRARIES
3 4456 0154373 9

ORNL/TM-10212

ornl

OAK RIDGE
NATIONAL
LABORATORY

MARTIN MARIETTA

Convective Contributions to Local Power Loss in a Bumpy Torus

S. Hiroe
B. H. Quon
G. R. Haste, Jr.
J. R. Goyer
J. S. Tolliver
L. Solensten
K. A. Connor

OAK RIDGE NATIONAL LABORATORY
CENTRAL RESEARCH LIBRARY
CIRCULATION SECTION
4500N ROOM 175
LIBRARY LOAN COPY
DO NOT TRANSFER TO ANOTHER PERSON
If you wish someone else to see this report, send in name with report and the library will arrange a loan.

OPERATED BY
MARTIN MARIETTA ENERGY SYSTEMS, INC.
FOR THE UNITED STATES
DEPARTMENT OF ENERGY

Printed in the United States of America. Available from
National Technical Information Service
U.S. Department of Commerce
5285 Port Royal Road, Springfield, Virginia 22161
NTIS price codes—Printed Copy: A03; Microfiche A01

This report was prepared as an account of work sponsored by an agency of the United States Government. Neither the United States Government nor any agency thereof, nor any of their employees, makes any warranty, express or implied, or assumes any legal liability or responsibility for the accuracy, completeness, or usefulness of any information, apparatus, product, or process disclosed, or represents that its use would not infringe privately owned rights. Reference herein to any specific commercial product, process, or service by trade name, trademark, manufacturer, or otherwise, does not necessarily constitute or imply its endorsement, recommendation, or favoring by the United States Government or any agency thereof. The views and opinions of authors expressed herein do not necessarily state or reflect those of the United States Government or any agency thereof.

ORNL/TM-10212
Dist. Category UC-20 f, g

Fusion Energy Division

CONVECTIVE CONTRIBUTIONS TO LOCAL POWER LOSS IN A BUMPY TORUS

S. Hiroe B. H. Quon*
G. R. Haste, Jr. J. R. Goyer†
J. S. Tolliver L. Solensten†
K. A. Connor†

*JAYCOR, Torrance, California 90503
†Rensselaer Polytechnic Institute, Troy, New York 12181

Date published: December 1986

Prepared by the
OAK RIDGE NATIONAL LABORATORY
Oak Ridge, Tennessee 37831
operated by
MARTIN MARIETTA ENERGY SYSTEMS, INC.
for the
U.S. DEPARTMENT OF ENERGY
under contract DE-AC05-84OR21400

MARTIN MARIETTA ENERGY SYSTEMS LIBRARIES
3 4456 0154373 9

CONTENTS

ABSTRACT v

I. INTRODUCTION 1

II. LIMITER EXPERIMENTS 1

III. DISCUSSION 8

A. Trapped particle fraction 8

B. Vacuum field drift orbits 8

C. Microwave power absorption 10

D. Electric field effects 11

IV. CONCLUSIONS 16

ACKNOWLEDGMENTS 18

REFERENCES 19

ABSTRACT

Power flow in the ELMO Bumpy Torus [*Plasma Physics and Controlled Nuclear Fusion Research (Tokyo, 1974)* (IAEA, Vienna, 1975) Vol. 2, p. 141; Plasma Phys. **25**, 597 (1983)] was investigated by measuring the power received by a limiter. Selective removal of heating power from various cavities, including the cavity with the limiter, has demonstrated that the majority of the power is lost locally. Observations of the potential structure demonstrate that asymmetric potential contours are present which can lead to enhanced plasma loss.

I. INTRODUCTION

A knowledge of power flow is of fundamental importance in understanding the performance of any plasma confinement system. Quantitative information about the various forms of power loss is essential in determining power balance. This information is also useful in evaluating the transport processes that affect plasma confinement.

Power flow in the ELMO Bumpy Torus (EBT)[1] was investigated by measuring the power received by a limiter for a number of heating configurations. These experiments have served to distinguish between the power which is lost locally, in a single sector of EBT, and that which propagates toroidally around the device. The majority of the power delivered to the plasma is lost locally, with the remainder distributed toroidally. The experimental evidence for the division of the power into these two categories is presented in Sec. II.

There are several possible causes for the preponderance of local loss, and these are listed in Sec. III, which is a discussion of the effects that could lead to the observed dominance of local power loss. Although it is not possible to determine the principal cause, the electric field can be a major contributor. This can result in direct loss by convection, or $\mathbf{E} \times \mathbf{B}$ drifts, as well as enhancing the diffusive loss. These conclusions rely on measurements using a heavy-ion beam probe (HIBP).[2] Development of this probe has resulted in detailed two-dimensional potential contours.[3] The effect of these potential distributions on equilibrium[4] and confinement[5] has been considered, and this paper treats the effects on power flow.

II. LIMITER EXPERIMENTS

The EBT device[6,7] consists of 24 cavities, as shown in Fig. 1. The labeling convention and a few of the diagnostic locations are shown in this figure. A pair of movable limiters (inboard and outboard) were installed in cavity S3 and were instrumented to measure the power received. The power measured by the limiters

ORNL-DWG 84-3736 FED

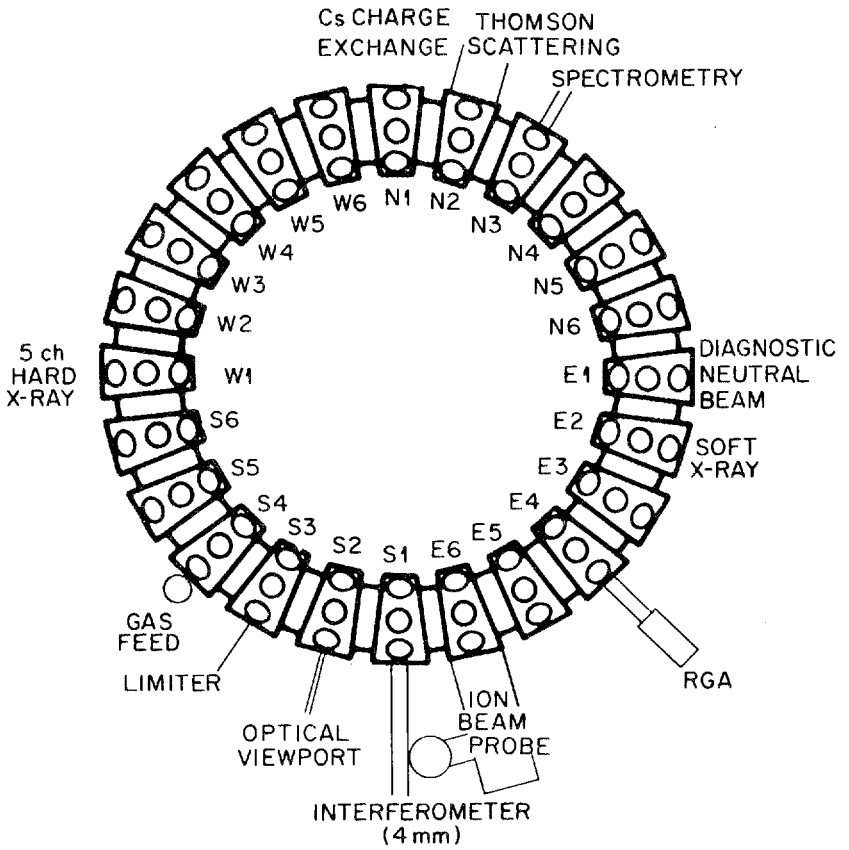

Fig. 1. Locations of some of the diagnostics on EBT-Scale.

is due to the plasma flux, and is insensitive to the radiated power, owing to the small solid angle subtended by the limiters. Radiated power can be a significant contribution to the power balance[8], particularly at the higher neutral densities.

The experiments described here used two different heating frequencies: 18 and 28 GHz. At 28 GHz, up to 200 kW is available from a gyrotron power source. This power enters a toroidal manifold (not shown in the figure) for distribution to each of the cavities, so the power distribution is fixed and not subject to experimental control. Typically, the magnetic field is 0.725 T when operating at 28 GHz. At 18 GHz, the power available is less (~50 kW) but the degree of experimental control

is greater. A set of four klystrons feeds a distribution system, with individual feeds and controls for each cavity. At this frequency, the central magnetic field is 0.5 T.

The operating positions of the limiters within S3 (shown in Fig. 2) are just outside the projection, along magnetic field lines, of the hot electron ring. Since the two limiters lie in the same plane, one cannot be inserted beyond its operating position if the other one is at its operating position. When the limiters are at their respective operating positions, the outer limiter receives roughly twice the power of the inner limiter. The difference is due to the relative positions of the two limiters: the inside limiter is just outside the flux line which grazes the mirror throat, the outer limiter is 3 cm inside the corresponding grazing flux line. This power difference was confirmed in a series of experiments in which the ratio was

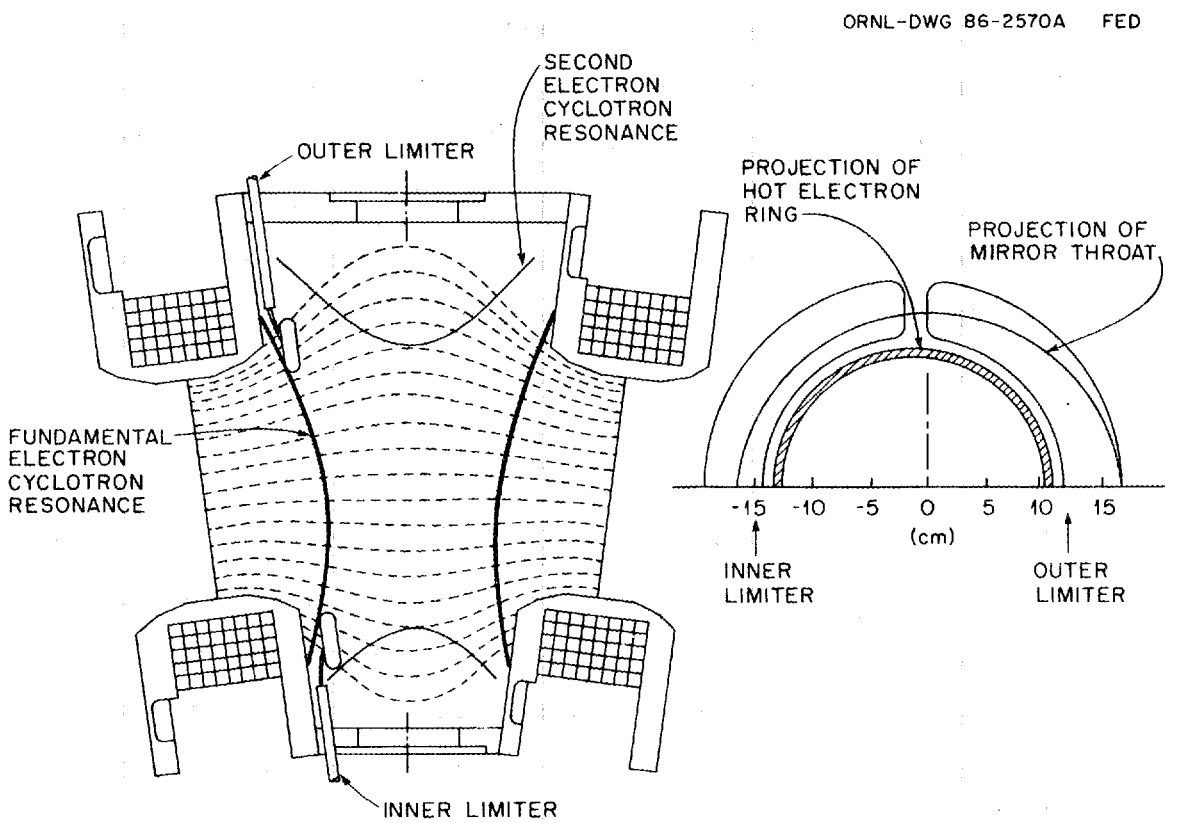

Fig. 2. Locations of the inner and outer limiters in an EBT cavity.

shown to be 2.5 ± 0.3 over a range of pressure and power. This ratio is important to the ensuing discussion because, for many of the experiments, only the power to the outer limiter was measured. The inner limiter power was estimated from this ratio.

The ability to control power distribution with the 18-GHz source was utilized in another series of experiments, where the outer limiter power was monitored as the microwave power to individual cavities was turned off. These data are shown in Fig. 3, where limiter power is plotted as a function of the cavity position where the microwave power is removed. The various curves in the figure are for different values of the ambient neutral pressure. As noted above, the fact that the magnitude of the limiter power is lowest at the highest pressure is due to the larger radiated power there, leaving less power for the plasma flux which strikes the limiter. At the extreme left of each curve, the power is plotted for the case when *all* cavities are fed. This figure shows that the limiter power is independent of the cavity position where the microwave power is removed, unless the microwave power is removed from the cavity where the limiter is located, when an additional power decrement is noted. These data suggest that the limiter power could be divided into two categories—locally lost power and that which travels around the torus. As mentioned previously, the inner limiter power was not measured in these experiments. To take that power into account, the outer limiter power is increased by 1/2.5 or 40%. The outer power can be expressed as

$$P(\text{outer}) = \frac{1}{1.4} \sum P_i(\text{tor}) + \frac{1}{2 \times 1.4} P(\text{local}) \quad , \tag{1}$$

where $P_i(\text{tor})$ is the microwave power absorbed in cavity i and which travels toroidally and $P(\text{local})$ is the microwave power absorbed per cavity which is lost without propagating around the torus. The factor of one-half that multiplies $P(\text{local})$ in Eq. (1) reflects the assumption that one-half of the locally lost power flows to the side of the cavity where the limiter is located, and the other half flows to the opposite side.

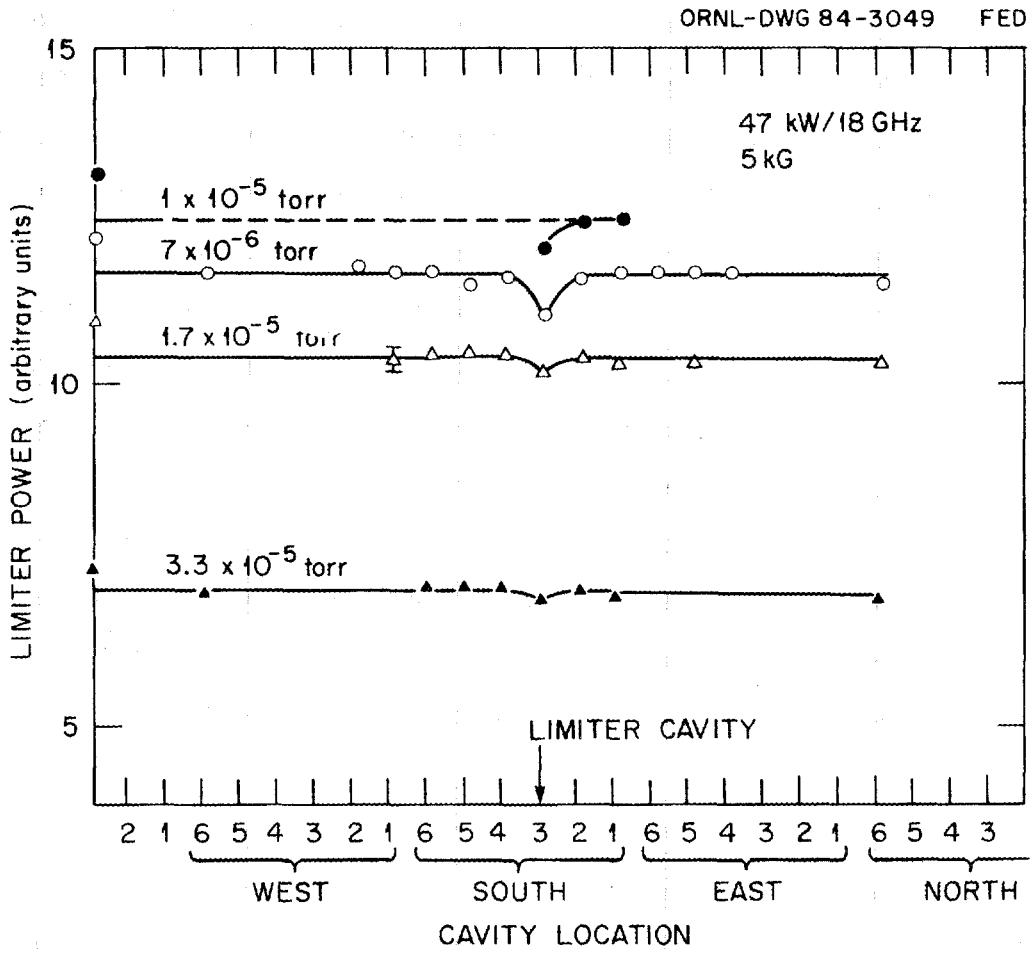

Fig. 3. Power received on the outer limiter as the microwave feed to different cavities is turned off. The limiter power when the microwave feed is into *all* of the cavities is indicated at the extreme left.

There is in Eq. (1) an implicit assumption that all of the power that flows toroidally from each of the cavities will impinge on the limiter. The data of Fig. 3 can be used to verify that this is indeed the case. The toroidal contribution to the limiter power can be written more explicitly in Eq. (2), where the factor of one-half reflects the fact that half of the toroidal power flows in each direction around the torus:

$$P_{\mathrm{lim,tor}} = \frac{1}{2}\sum P_i(\mathrm{tor})\{\exp(-|1-i|\alpha) + \exp(-|24-(1-i)|\alpha)\} \quad . \qquad (2)$$

The summation is over i, where i is an index denoting the cavity number. The limiter is located in cavity 1, and α is the attenuation factor for the toroidal

power, expressed in reciprocal cavity numbers. This factor (α) is proportional to the perpendicular-to-parallel conductivity ratio, and so is expected to be small.

The value of α can be determined, in principle, from the slope of the curves in Fig. 3. Although the curves are drawn with a slope of zero, it is possible to estimate the *largest* slope of the line that is consistent with the data. This estimate leads to an α value of $<3 \times 10^{-3}$. A separate determination of α led to an α value of $<7 \times 10^{-3}$. In that experiment the power was measured on a Faraday shield for an ion cyclotron resonance heating (ICRH) antenna[9] as the limiter was inserted to intersect the field lines leading to the Faraday shield.

With such a small value for the attenuation factor, it is possible to pass to the limit $\alpha = 0$ with little error, and then Eq. (1) is a valid expression for the power received by the limiter. Figure 3 can then be analyzed to determine the relative amount of power lost locally. In describing this analysis it is useful to define some quantities:

P_{24} is the power received by the limiter when all 24 cavities are fed (represented by the points at the extreme left in Fig. 3).

P_{23} is the power received by the limiter when the power is removed from a cavity that does *not* contain the limiter (represented by the straight lines in the figure).

P_{lc} is the power received by the limiter when the power is removed from the limiter cavity (the lowest point on each of the curves).

Then

$$P_i(\text{tor}) = (P_{24} - P_{23}) \times 1.4$$

$$P(\text{local}) = (P_{23} - P_{lc}) \times 2 \times 1.4$$

$$f(\text{local}) = P(\text{local})/[P_i(\text{tor}) + P(\text{local})] \quad .$$

The analysis is summarized in Table I, which shows that more than half the power in each cavity is lost locally and does not travel toroidally. These data show that the local fraction increases at the lowest pressure. This increase may be due to the formation of two populations of low pressure which should lose their energy locally:

TABLE I. Local loss fraction calculated from Fig. 3

Pressure (torr)	P_{24}	P_{23}	P_{lc}	P_i(tor)	P(local)	f(local)
7.0×10^{-6}	12.1	11.6	11.0	0.7	1.6	0.69
1.0×10^{-5}	13.1	12.4	12.0	0.9	1.0	0.53
1.7×10^{-5}	10.9	10.4	10.1	0.7	0.6	0.45
3.3×10^{-5}	7.3	7.0	6.8	0.4	0.4	0.52
					Average =	0.55 ± 0.10

hot and warm electrons. The hot electrons, which form a ring, are primarily lost by small angle scattering, and so tend to be wiped off on the limiters before they can scatter into the passing particle population. The warm electrons, which are a "seed" population for the hot electrons, are heated near the mirrors. As discussed in Sec. III.C, this heating process results in an enhanced local power loss.

The previous discussion is based on the assumption that there are only two loss channels for the power introduced into a cavity: into plasma which is either lost locally or which travels toroidally. There is, however, another loss channel that has been neglected. Some of the power can "leak" into the adjacent cavity before being absorbed. In general, this leakage power is small, but under some conditions it can be as much as 20%.[10] Leakage at that level would increase the local fraction calculated in the table to 0.6 ± 0.1.

This analysis utilized the flexibility of the 18-GHz microwave distribution system to make measurements of the relative powers to the limiters as the feed to selected cavities, including the limiter cavity, was turned off. The absolute limiter power was *not* determined for these experiments. However, some measurements were made with 28-GHz power, where the opposite situation occurred: absolute limiter power determinations were made, but it was not possible to turn off the power to individual cavities. If one estimates the local power loss fraction from the ratio of the limiter to absorbed power for the 28-GHz experiments, then one obtains a locally lost fraction of ~75%, so the local power loss is dominant for that case as well.

III. DISCUSSION

As demonstrated in Table I, more than half the power absorbed in each cavity is lost locally and does not travel toroidally. The question naturally arises as to how this fraction compares with that expected. In this section several estimates of the local fraction will be made. Each of the estimates has an aspect which makes it of questionable applicability, but each shows that the local loss should be dominant. The estimates include effects of single particle confinement (A and B), of heating near the loss region (C), and of electric field enhancement of both diffusive and convective losses (D). Although each of these may contribute, electric field effects are clearly important.

A. Trapped particle fraction

For an isotropic distribution the trapped particle fraction is given by

$$\frac{n_t}{n} = 1 - \frac{1}{\sqrt{M}} \quad ,$$

which is 0.73 for a mirror ratio (M) of 1.9, the on-axis value for EBT. If the loss rates for the trapped and passing populations were the same, then one would expect ~73% of the power to be lost locally. One would expect the two rates to be the same if the confinement were dominated by convection, or $\mathbf{E} \times \mathbf{B}$ drifts, as discussed in Sec. III.D.

This gives a questionable estimate for the local power fraction because the EBT plasma is known to have a non-Maxwellian energy distribution in which the higher energy portion is anisotropic.

B. Vacuum field drift orbits

Drift orbits have been calculated for the magnetic fields of EBT by finding the surfaces of the invariant $J(= \int v_{\|} dl)$. These surfaces, and therefore the drift orbits, differ for different pitch angles. The drift orbits for small pitch angles are nearly

circular, while those for larger pitch angles become elongated and many of them intersect the walls at the coil throats. Thus the confinement for these particles is poorer than for those with small pitch angles. To make this comparison of the confinement properties more quantitative, a "volumetric efficiency" is defined as the ratio of the area of the largest drift orbit that does not hit the wall to the area of the projection of the coil throat. This quantity is shown as a function of pitch angle in Fig. 4. The fraction of the plasma cross section is much smaller for passing particles than for trapped particles, but that available for transitional particles (between trapped and passing) is smaller yet.

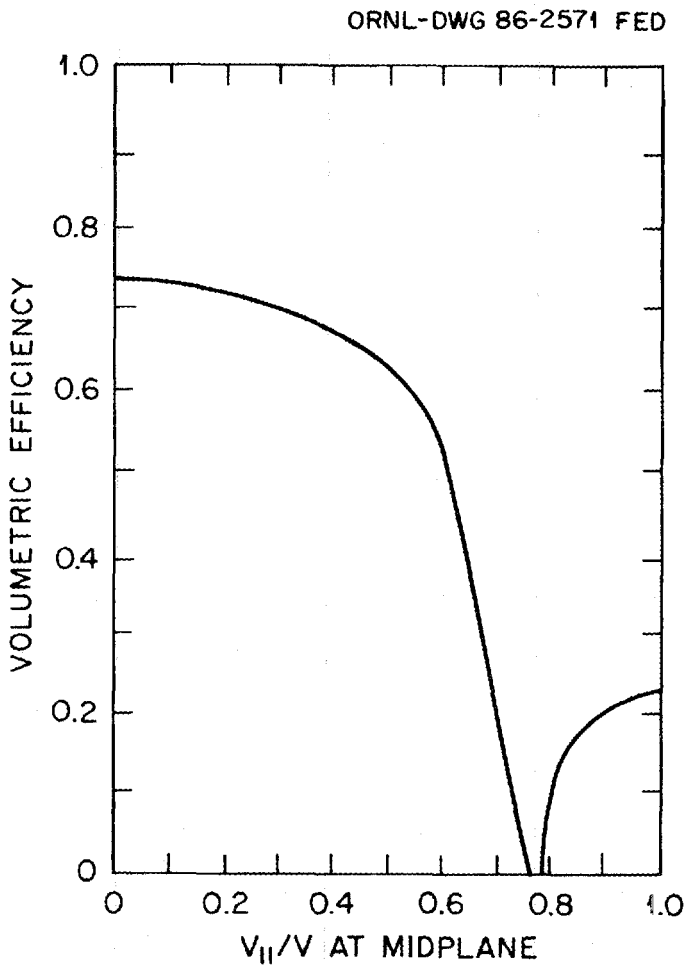

Fig. 4. The fraction of the projection of the coil throat ("clear bore") in which the drift surfaces are closed, as a function of the particle pitch angle.

This indicates that, of the power absorbed by the plasma, only that absorbed near the center has a chance of propagating toroidally, for near the center is the only region where passing particles can exist. For the situation appropriate to Fig. 4, fewer than 30% of the passing particles qualify.

This estimate has two serious problems. First, there is no assurance that the incident power is absorbed uniformly over the plasma cross section. Second, the ambipolar electric field affects the confinement profoundly. The effect for high energy particles ($e\phi/kT \ll 1$) is negligible; for low energy particles ($e\phi/kT \gg 1$) it is the dominant effect. Thus, it is important to know both where the power is absorbed and which energy group receives the power.

The effects on confinement properties for a *symmetric* potential (ad hoc) have been reported by Fujiwara et al.[11] For $kT/e\phi \leq 4$, the confinement for both electrons and ions is improved, with the result that the 30% value for passing particles mentioned above increases to ~50%. The effects for an *asymmetric* potential have not been investigated in the same detail, but they are likely to reduce the region available to passing particles still further.

C. Microwave power absorption

Some recent calculations by Batchelor[12] have led to a better understanding of the spatial distribution of the power absorbed as well as the principal particle groups that receive the power. Ray tracing techniques have demonstrated that the microwave electric field strength reaches its maximum near the high field region of the coil throats. Specifically, this maximum occurs where the field strength is greater than the resonance value.

The particles that absorb the power, then, are those for which the Doppler shifted resonance is valid: $\omega = \omega_c \pm k_{\|}v_{\|}$. This requires that (1) the particles go beyond the resonant surface and penetrate into the throat region and (2) the particles' energy be high so that the Doppler shift ($k_{\|}v_{\|}$) is large. As noted above, the particles that turn near the mirror throat are the most poorly confined, so

this heating method is particularly inefficient. This evaluation relies on *magnetic* confinement, so electric field effects have not been included. The calculation could be expected to be valid near the center of the plasma, where the potential contours are closed and convective effects do not lead to losses. In that region, roughly half the power absorbed could be quickly lost by poorly confined particles.[13]

D. Electric field effects

As noted previously, the electric field can be the dominant influence on particle motion at low energies. As a result, the electric field—and particularly its symmetry—will have a profound effect on confinement.[14] Roughly, one can say that the electric field effects become dominant when the $\mathbf{E} \times \mathbf{B}$ drifts exceed the gradient drifts,

$$\frac{E}{B} > \frac{T_e}{eRB} \qquad \text{or} \qquad E > \frac{T_e}{eR} \,. \tag{3}$$

If the major radius R is chosen to be 1.5 m, then the critical field is 33 V/m for a 50-eV population. In fact, it is the *asymmetric* part of the electric field which must exceed this value, since the purely radial component only results in a poloidal drift.

The dominance of the electric field is clearly obvious in the high neutral pressure regime known as the C-mode. The potential distribution as determined by HIBP is shown in Fig. 5 for this regime. In this case the electric field is certainly *not* cylindrically symmetric. The nearly horizontal equipotential surfaces are equivalent to a vertical electric field, which is the classic result of toroidal confinement in a device without rotational transform. The equipotential surfaces also represent streamlines for plasma flow due to the $\mathbf{E} \times \mathbf{B}$ drift. The plasma lifetime due to this flow can be estimated as $\tau = aB/E$. For an average magnetic field (B) of 0.75 T, a characteristic plasma size (a) of 0.12 m, and an electric field (E) of 1500 V/m, a lifetime of 60 μs results, which agrees well with the ionization time for these conditions. Since this loss rate is even more rapid than that due to Bohm diffusion, the contention that the electric field dominates the confinement is well founded.

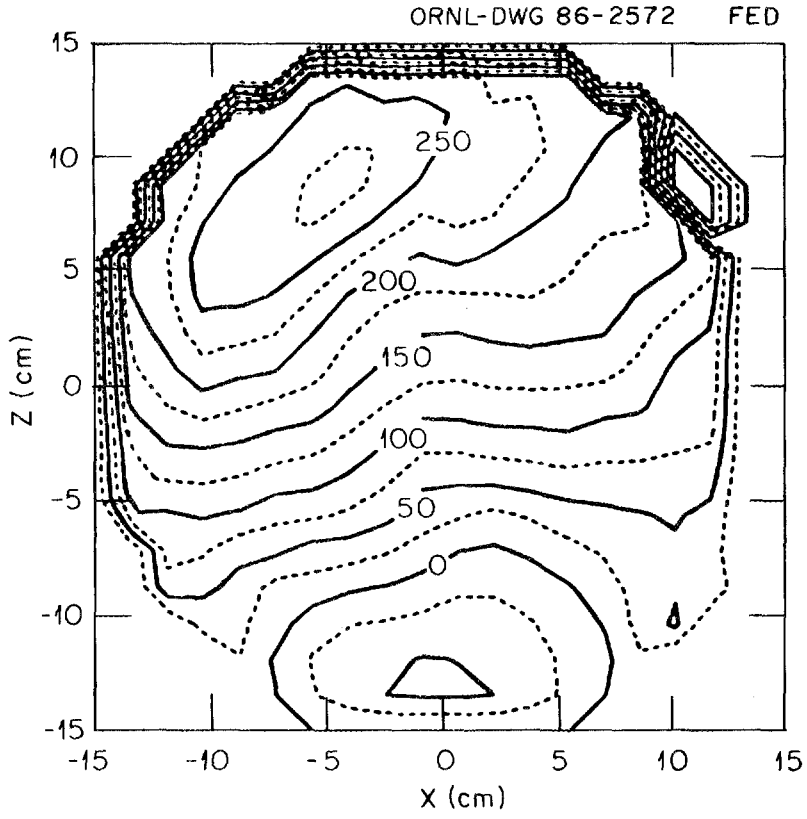

Fig. 5. EBT potential distribution, as determined by heavy ion beam probing, in the C-mode.

The topology of the potential contours changes significantly as the neutral pressure is reduced[5], as shown in Fig. 6. In this regime, known as the T-mode, the potential has a symmetric plus an asymmetric component, such that the asymmetry results in a horizontal electric field.

The asymmetry is made more apparent by plotting the potential along the horizontal midplane, as shown in Fig. 7. The potential is greater on the inside of the device than on the outside, so a net horizontal electric field results, with a magnitude of ~500 V/m. Using the criterion of Eq. (3), this horizontal field will have a dominant effect on particles of less than 750 eV, which certainly constitute the bulk of the plasma, for which $T_e < 100$ eV.[15]

As discussed previously, the electric field leads to convective losses ($\mathbf{E} \times \mathbf{B}$) in the C-mode. Convection is also an important loss in the T-mode because the closed

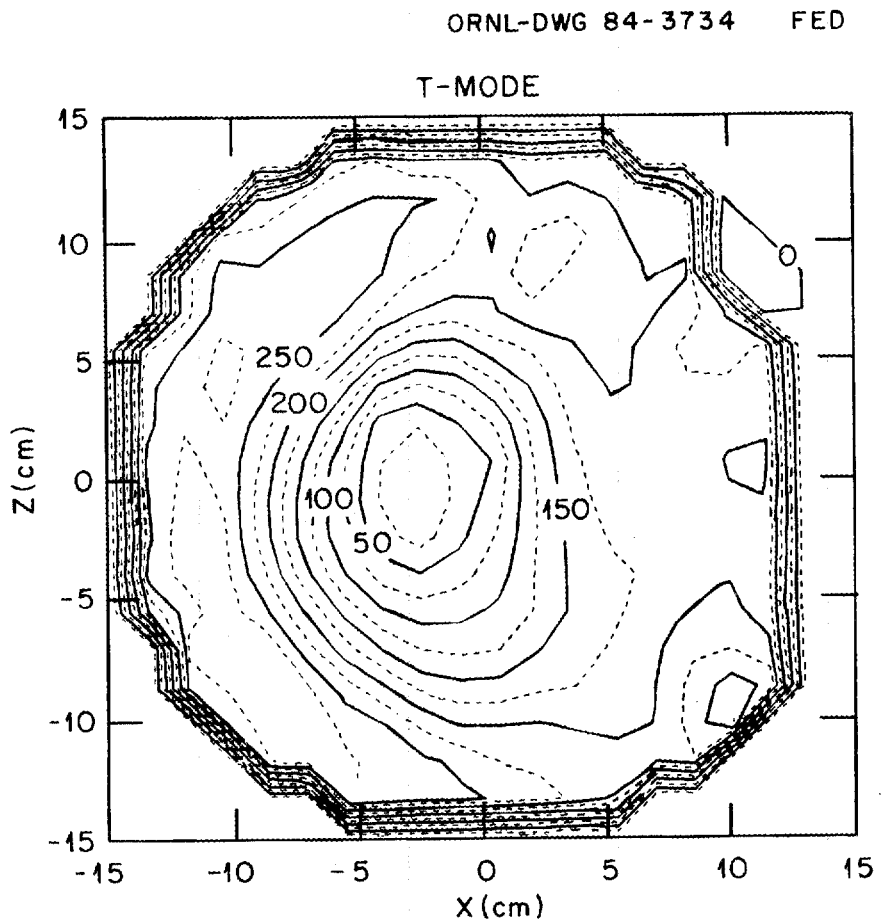

Fig. 6. EBT potential distribution in the T-mode.

potential surfaces occur only near the plasma center. In the outer regions, which constitute the bulk (~70%) of the plasma, the potential surfaces are open so that plasma can flow along those surfaces to the wall.

One can also expect that diffusive losses will be strongly affected by the electric field, since the diffusion coefficient directly involves the vertical drifts:

$$D \sim \frac{\nu}{\nu^2 + \Omega^2} \left(v_y\right)^2 \ , \tag{4}$$

and

$$v_y = v_{\nabla B} + v_{\mathbf{E_h} \times \mathbf{B}} + v_{\delta B} \ , \tag{5}$$

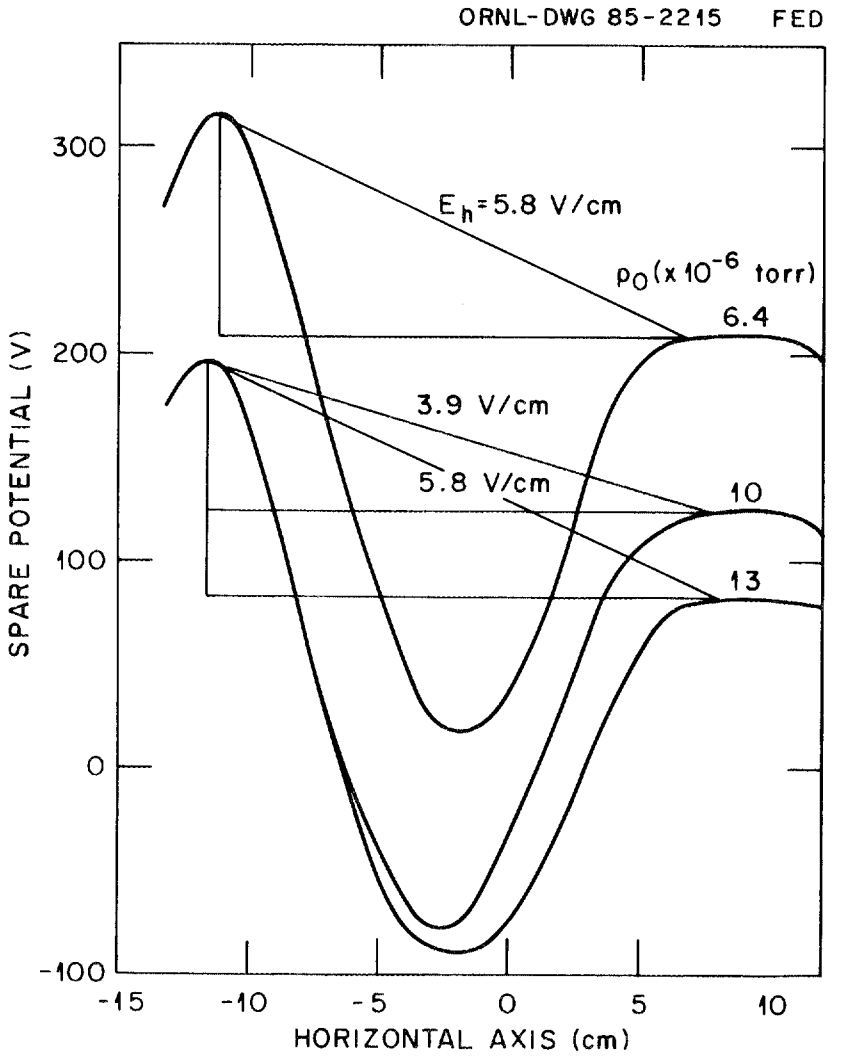

Fig. 7. EBT potential distribution along the major radius.

where ν is the collision frequency, Ω is the precessional frequency ($\mathbf{E} \times \mathbf{B}$ and ∇B), v_y is the vertical drift velocity, $\mathbf{E}_h$ is the electric field horizontal component, and δB is the error field.

In the notation of Eq. (5) the horizontal component of the electric field enters explicitly. Since the electric field term can be as much as an order of magnitude greater than the gradient drift term, one might expect the diffusive losses to be two orders greater than the neoclassical values. The neoclassical lifetime[16,17] is expected to be ~10 ms, so the horizontal electric field effects could reduce the actual lifetime to ~100 μs.

The third term on the right of Eq. (5) is due to field errors:

$$v_{\delta B} = v_{\parallel} \frac{\delta B}{B} , \tag{6}$$

where $v_{\parallel}$ is the velocity parallel to the magnetic field line.

The effects of the field errors on the diffusive losses should be either negligible or dominant depending on whether $v_{\delta B}$ is less than or greater than $v_{\mathbf{E_h} \times \mathbf{B}}$. For a 50-eV plasma and $\mathbf{E_h} = 500$ V/m, the critical error field level is $\delta B/B = 1.6 \times 10^{-4}$. Figure 8 shows the power received by the limiter as the field error level is varied, using a pair of coils outside the vacuum vessel. Little change in the limiter power occurs as a vertical error field is applied, with current through a horizontal coil pair. However, changes in the limiter power are seen when the horizontal field error reaches a value $\sim 10^{-4}$, which agrees with the discussion above.

A Monte Carlo calculation[18] of the confinement properties of the bumpy torus has reinforced concern about the deleterious effects of asymmetric potential structures. In that calculation the potential was chosen to be (1) constant on surfaces of

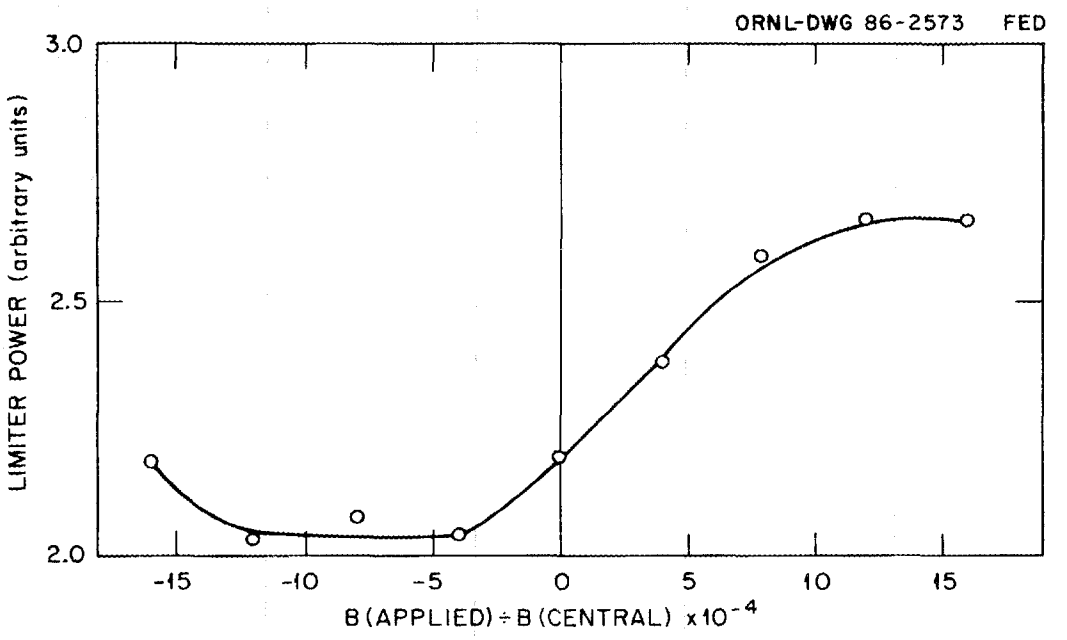

Fig. 8. Variation of the limiter power vs the externally applied error field. An applied (fractional) field of about -5×10^{-4} compensates for the inherent field errors in the device.

constant $\int dl/B$, so that it had the same symmetry as those surfaces, or (2) distorted from that basic configuration by a cos Θ perturbation of controllable amplitude. When the perturbation vanished the calculated lifetime was just the neoclassial value. When the perturbation was increased to the level of the actual potential asymmetry, the particles were lost about 100 times faster. The results are shown in Fig. 9. The potential structure and the plasma distribution are shown in Fig. 9a for a symmetric potential and in Fig. 9b for the asymmetric case, which is close to the experimental distribution. It should be noted that the actual potential structure is centered further out than the minimum of the $\int dl/B$ surfaces, so the simulation is not entirely realistic. The effects of the asymmetry, however, are striking and consistent with the discussion above.

There are two possible explanations for the asymmetry of the potential structure. One[19] is that the asymmetry of the drift orbits, particularly of the transitional particles, results in an asymmetric population of warm electrons. These warm electrons determine the potential structure, which must then necessarily be asymmetric. The second explanation[4,20,21] is that a horizontal electric field is required to give the force balance for equilibrium in a toroidal device without rotational transform. These two have very different consequences for future devices. If the first is correct, then drift orbit symmetrization, as achieved by the design of the ELMO Bumpy Square (EBS) device,[19] would result in symmetrization of the potential and much better confinement. If the second is valid, then a horizontal electric field is a necessary consequence of toroidal closure of the magnetic field lines, and little improvement in confinement could be expected for a device with more symmetric drift orbits.

IV. CONCLUSIONS

A pair of movable limiters in one sector of EBT has permitted a determination of the fraction of the absorbed power that is lost locally. This fraction, ~60%,

ORNL-DWG 86-2653 FED

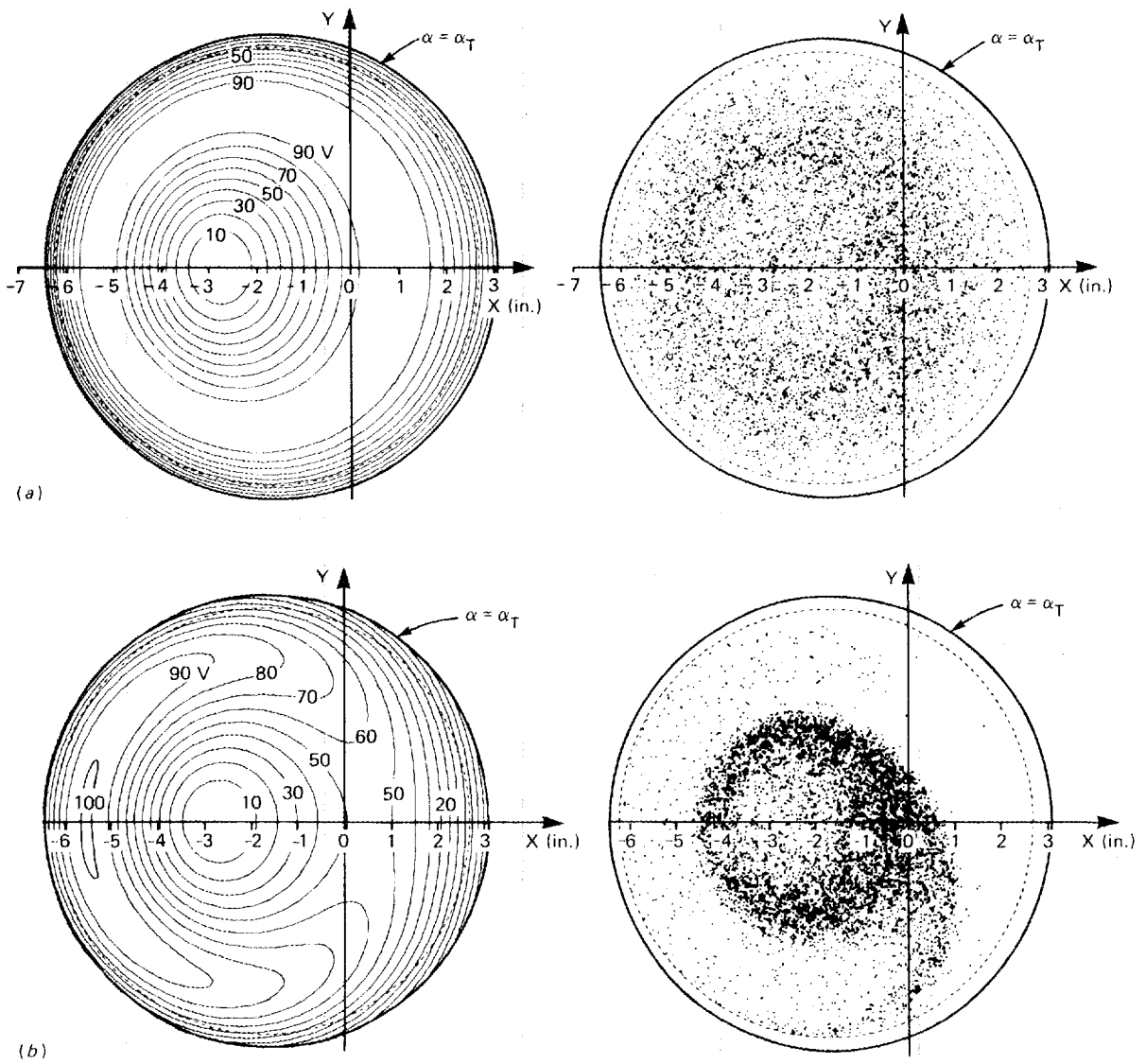

Fig. 9. Results of a Monte Carlo calculation of the effects of the potential structure. The potential structure is shown at the left, and a series of "snapshots" of the particle locations is superimposed on the right. (a) A symmetric case. (b) Results for an asymmetric potential, which simulates the experimental observations.

is approximately equal to that expected from several estimates. In each of these estimates the electric field plays a critical role.

(1) To relate the local power loss fraction to the trapped particle fraction, one has to assume that the loss rates for the trapped and passing particles are the same. This would be the case if the confinement were dominated by convection *or* by diffusion.

(2) The vacuum drift orbits are profoundly affected by the electric field. The fraction of the plasma cross section available to passing particles is about 30% for the case with no electric field effects. With an electric field, low energy particles ($E < e\phi$, which constitute the bulk of the plasma) are constrained to drift along equipotential surfaces. Those surfaces are closed in only about the central 25% of the plasma cross section.

(3) The estimates of the power loss caused by heating particles near the loss cone are only valid for the region where the equipotential surfaces are closed (25% of the plasma cross section).

Thus, for several reasons it is clear that the dominant contribution to power loss in EBT is due to the asymmetric electric field, which results in convection in the outer region, and can also enhance diffusive losses in the central region. As a result, the lifetime is shorter than the neoclassical value.

ACKNOWLEDGMENTS

The authors thank the members of the EBT experimental staff for their help with these experiments. Thanks are also due R. Juhala of the McDonnell Douglas Astronautics Company for the limiter used in these experiments, L. W. Owen for the drift orbit calculations, and D. B. Batchelor and D. W. Swain for discussions.

This research was sponsored by the Office of Fusion Energy, U.S. Department of Energy, under Contract No. DE-AC05-84OR21400 with Martin Marietta Energy Systems, Inc.

REFERENCES

1. R. A. Dandl, H. O. Eason, A. C. England, G. E. Guest, C. L. Hedrick, H. Ikegami, and D. B. Nelson, in *Plasma Physics and Controlled Nuclear Fusion Research (Tokyo, 1974)* (IAEA, Vienna, 1975) Vol. 2, p. 141.
2. P. L. Colestock, K. A. Connor, R. L. Hickok, and R. A. Dandl, Phys. Rev. Lett. **40**, 1717 (1978);
3. F. M. Bieniosek and K. A. Connor, Phys. Fluids **26**, 2256 (1983).
4. S. Hiroe, J. A. Cobble, R. J. Colchin, G. L. Chen, K. A. Connor, J. R. Goyer, and L. Solensten, Phys. Fluids **29**, 1659 (1986).
5. S. Hiroe, J. C. Glowienka, D. L. Hillis, J. B. Wilgen, G. L. Chen, J. A. Cobble, A. M. El-Nadi, J. R. Goyer, L. Solensten, W. H. Casson, O. E. Hankins, and B. H. Quon, to be published in Phys. Fluids **30**, 848 (1987).
6. R. A. Dandl, H. O. Eason, A. C. England, G. E. Guest, C. L. Hedrick, and J. C. Sprott. See National Technical Information Service Document ORNL/TM-3694 (Oak Ridge National Laboratory Report ORNL/TM-3694). Copies may be obtained from the National Technical Information Service, Springfield, Virginia 22161. The price is $8.00 plus a $3.00 handling fee. All orders must be prepaid.
7. R. J. Colchin, T. Uckan, F. W. Baity, L. A. Berry, F. M. Bieniosek, L. Bighel, W. A. Davis, E. Dullni, H. O. Eason, J. C. Glowienka, G. A. Hallock, G. R. Haste, D. L. Hillis, A. Komori, T. L. Owens, R. K. Richards, L. Solensten, T. L. White, and J. B. Wilgen, Plasma Phys. **25**, 597 (1983) (and references listed therein).
8. D. H. McNeill, Plasma Physics and Controlled Fusion **28**, 717 (1986).
9. F. W. Baity and T. L. Owens, Nucl. Fusion **23**, 49 (1983).
10. D. B. Batchelor, R. C. Goldfinger, and D. A. Rasmussen, Phys. Fluids **27**, 948 (1984).
11. M. Fujiwara, T. Kamimura, M. Hosokawa, T. Shoji, H. Iguchi, H. Sanuki, M. Aizawa, T. Takasugi, F. Tsuboi, H. Tsuchidate, K. Matsunaga, K. Kadota,

A. Tsushima, K. W. Whang, and H. Ikegami, in *Plasma Physics and Controlled Nuclear Fusion Research (Baltimore, 1982)*, (IAEA, Vienna, 1983) Vol. 2, p. 197.

12. D. B. Batchelor, in *Proceedings of the 4th International Symposium on Heating in Toroidal Plasmas* (International School of Plasma Physics, Varenna, 1984), Vol. II, p. 779.
13. D. B. Batchelor (private communication).
14. A. M. El-Nadi, Phys. Fluids **28**, 878 (1985).
15. J. A. Cobble, Rev. Sci. Instrum. **56**, 73 (1985), J. A. Cobble, Rev. Sci. Instrum. **56**, 1018 (1985).
16. E. F. Jaeger, D. A. Spong, and C. L. Hedrick, Phys. Rev. Lett. **40**, 866 (1978).
17. D. E. Hastings and J. S. Tolliver, Phys. Fluids **29**, 193 (1986).
18. J. S. Tolliver and C. L. Hedrick, to be published in Phys. Fluids (March 1987).
19. C. L. Hedrick and L. W. Owens, to be published in Phys. Fluids (March 1987).
20. D. G. Bulyginskii, V. S. Yuferev, and E. V. Galaktionov, Sov. J. Plasma Phys. **3**, 528 (1977).
21. N. G. Popkov, Sov. J. Plasma Phys. **5**, 482 (1979).

ORNL/TM-10212
Dist. Category UC-20 f,g

INTERNAL DISTRIBUTION

1. R. D. Burris
2. G. L. Chen
3. R. J. Colchin
4. J. C. Glowienka
5–6. G. R. Haste
7. D. L. Hillis
8–12. S. Hiroe
13. D. Rasmussen
14. J. Sheffield
15–16. J. S. Tolliver
17. J. R. Wilgen
18–19. Laboratory Records Department
20. Laboratory Records, ORNL-RC
21. Document Reference Section
22. Central Research Library
23. Fusion Energy Division Library
24. Fusion Energy Division Publications Office
25. ORNL Patent Office

EXTERNAL DISTRIBUTION

26–27. B. H. Quon, Applied Microwave Plasma Concepts, Inc., Encinitas, CA 92024

28–29. J. R. Goyer, Physics International, San Leandro, CA 94577

30–32. L. Solensten, Grumman Aeronautics Corp., Bethpage, NY 11714

33. Office of the Assistant Manager for Energy Research and Development, U.S. Department of Energy, Oak Ridge Operations, P. O. Box E, Oak Ridge, TN 37831

34. J. M. Turner, Office of Fusion Energy, Office of Energy Research, ER-522 Germantown, U.S. Department of Energy, Washington, DC 20545

35. M. Fujiwara, Institute of Plasma Physics, Nagoya University, Nagoya 464, Japan

36. T. V. George, Plasma Technologies Branch, Division of Development and Technology, Office of Fusion Energy, Office of Energy Research, ER-531 Germantown, U.S. Department of Energy, Washington, DC 20545

37. T. Shoji, Institute of Plasma Physics, Nagoya University, Nagoya 464, Japan

38. A. Komori, Interdisciplinary Graduate School of Engineering Sciences, Kyushu University, Kasuga, Fukuoka 816, Japan

39. N. A. Krall, JAYCOR, P.O. Box 85154, San Diego, CA 92138

40. S. Hamasaki, JAYCOR, P.O. Box 85154, San Diego, CA 92138

41. N. H. Lazar, TRW Defense and Space Systems, One Space Park, Bldg. R-1, Redondo Beach, CA 92078

42. J. B. McBride, Science Applications International Corp., 1200 Prospect St., P.O. Box 2351, La Jolla, CA 92038
43. W. B. Ard, McDonnell Douglas Astronautics Company, Bldg. 278, P.O. Box 516, St. Louis, MO 63166
44. H. L. Berk, Institute for Fusion Studies, University of Texas at Austin, RLM 11.218, Austin, TX 78712
45. F. M. Bieniosek, McDonnell Douglas Astronautics Company, Bldg. 278, P.O. Box 516, St. Louis, MO 63166
46. R. A. Dandl, Applied Microwave Plasma Concepts, Inc., 2210 Encinitas Blvd., Suite P, Encinitas, CA 92024
47. R. S. Post, Plasma Physics Laboratory, Princeton University, P.O. Box 451, Princeton, NJ 08544
48. D. H. McNeill, Plasma Physics Laboratory, Princeton University, P.O. Box 451, Princeton, NJ 08544
49. K. Mizuno, Applied Science Dept., University of California-Davis, 228 Walker Hall, Davis, CA 95617
50. F. L. Ribe, College of Engineering, AERL Building, FL-10, University of Washington, Seattle, WA 98195
51. T. C. Simonen, Lawrence Livermore National Laboratory, P.O. Box 5511, Livermore, CA 94550
52. H. Weitzner, Associate Director, New York University, Courant Institute of Mathematical Sciences, 251 Mercer Street, New York, NY 10012
53. K. Tsang, Science Applications International Corp., 934 Pearl St., Boulder, CO 80302
54. B. Fried, Department of Physics, University of California, Los Angeles CA 90024
55. J. W. Van Dam, Institute for Fusion Studies, University of Texas at Austin, Austin, TX 78712
56. A. Wong, Department of Physics, University of California, Los Angeles CA 90024
57. H. Geode, R1/2144. TRW Inc., Energy Development Group, One Space Park, Redondo Beach, CA 90278
58. H. K. Forsen, Bechtel Group, Inc., Research Engineering, P.O. Box 3965, San Francisco, CA 94105
59. J. R. Gilleland, GA Technologies, Inc., Fusion and Advanced Technology, P.O. Box 81608, San Diego, CA 92138
60. R. A. Gross, Plasma Research Laboratory, Columbia University, New York, NY 10027
61. D. M. Meade, Princeton Plasma Physics Laboratory, P.O. Box 451, Princeton, NJ 08544
62. F. Prevot, CEN/Cadarache, Department de Recherches sur la Fusion Controlee, 13108 Saint-Paul-lez-Durance Cedex, France

63. M. Roberts, International Programs, Office of Fusion Energy, Office of Energy Research, ER-52 Germantown, U.S. Department of Energy, Washington, DC 20545
64. W. M. Stacey, Jr., School of Nuclear Engineering and Health Physics, Georgia Institute of Technology, Atlanta, GA 30332
65. D. Steiner, Rensselaer Polytechnic Institute, Nuclear Engineering Department, NES Building, Tibbets Avenue, Troy, NY 12181
66. R. Varma, Physical Research Laboratory, Navrangpura, Ahmedabad 380009, India
67. R. W. Conn, School of Chemical, Nuclear, and Thermal Engineering, Boelter Hall, University of California, Los Angeles, CA 90024
68. J. D. Callen, Department of Nuclear Engineering, University of Wisconsin, Madison, WI 53706-1687
69. D. D. Ryutov, Institute of Nuclear Physics, Siberian Branch of the Academy of Sciences of the U.S.S.R., Sovetskaya St. 5, 630090 Novosibirsk, U.S.S.R.
70. S. O. Dean, Fusion Power Associates, 2 Professional Drive, Suite 248, Gaithersburg, MD 20879
71. G. A. Eliseev, I. V. Kurchatov Institute of Atomic Energy, P.O. Box 3402, 123182 Moscow, U.S.S.R.
72. V. A. Glukhikh, Scientific-Research Institute of Electro-Physical Apparatus, 188631 Leningrad, U.S.S.R.
73. N. A. Davies, Office of the Associate Director, U.S. Department of Energy, Office of Fusion Energy, Office of Energy Research, ER-51 Germantown, Washington, DC 20545
74. G. G. Gibson, Westinghouse Electric Corp., Waltz Mill Site, P.O. Box 158, Madison, PA 15663
75. R. W. Gould, Department of Applied Physics, California Institute of Technology, Pasadena, CA 91125
76. D. G. McAlees, Exxon Nuclear Company, Inc., 777 106th Avenue NE, Bellevue, WA 98009
77. J. F. Clarke, Associate Director for Fusion Energy, Office of Energy Research, ER-50 Germantown, U.S. Department of Energy, Washington, DC 20545
78. D. B. Nelson, Acting Director, Division of Applied Physics, Energy Research, ER-50 Germantown, U.S. Department of Energy, Washington, DC 20545
79. Documentation SIGN, Departement de la Physique du Plasma et de la Fusion Controlee, Association EURATOM-CEA, Centre d'Etudes Nucleaires, B.P. 85, Centre du Tri, 38041 Grenoble Cedex, France
80. Bibliotheque, Service du Confinement des Plasmas, CEA, B.P. 06, 92 Fontenay-aux-Roses (Seine), France

81. Bibliothek, Institut fur Plasmaphysik, KFA, Postfach 1913, D-5170 Julich, Federal Republic of Germany
82. Bibliothek, Max-Planck Institut fur Plasmaphysik, D-8046 Garching, Federal Republic of Germany
83. Bibliotheque, Centre de Recherches en Physique des Plasmas, 21 Avenue des Bains, 1007 Lausanne, Switzerland
84. Library, Culham Laboratory, UKAEA, Abingdon, Oxfordshire, OX14 3DB, England
85. Library, FOM Instituut voor Plasma-Fysica, Rijnhuizen, Edisonbaan 14, 3439 MN Nieuwegein, The Netherlands
86. Library, Institute of Plasma Physics, Academia Sinica, Beijing, Peoples Republic of China
87. Library, Institute for Plasma Physics, Nagoya University, Nagoya 464, Japan
88. Library, International Centre for Theoretical Physics, Trieste, Italy
89. Library, Laboratorio Gas Ionizzati, CP 56, I00044 Frascati, Rome, Italy
90. Library, Plasma Physics Laboratory, Kyoto University, Gokasho, Uji, Kyoto, Japan
91. Plasma Research Laboratory, Australian National University, P.O. Box 4, Canberra, ACT 2000, Australia
92. Thermonuclear Library, Japan Atomic Energy Research Institute, Tokai Establishment, Tokai-mura, Naka-gun, Ibaraki-ken, Japan

93–278. Given distribution as shown in TIC-4500, Magnetic Fusion Energy (Distribution Category UC-20f,g: Theoretical Plasma Physics and Experimental Plasma Physics)